THE JOURNAL OF PHYSICAL CHEMISTRY B

Article

pubs.acs.org/JPCB

Formation of Polyelectrolyte Multilayers by Flexible and Semiflexible Chains

Bo Wu,[†] Chunliang Li,[†] Haiyang Yang,[‡] Guangming Liu,*[,†] and Guangzhao Zhang[§]

[†]Hefei National Laboratory for Physical Sciences at the Microscale, Department of Chemical Physics, University of Science and Technology of China, Hefei, P. R. China 230026

[‡]Department of Polymer Science and Engineering, University of Science and Technology of China, Hefei, P. R. China 230026

[§]Faculty of Materials Science and Engineering, South China University of Technology, Guangzhou, P. R. China 510640

Supporting Information

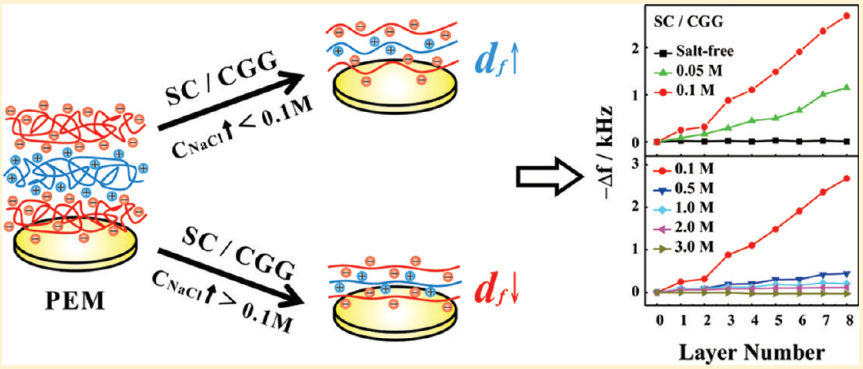

ABSTRACT: Poly(sodium 4-styrene sulfonate) (PSS) and poly(diallyldimethylammonium chloride) (PDDA) are flexible polyelectrolytes, whereas sulfated chitosan (SC) and cationic guar gum (CGG) are semiflexible polyelectrolytes. By use of a quartz crystal microbalance with dissipation (QCM-D), a zeta potential analyzer (ZPA), and atomic force microscopy (AFM), we have investigated the growth of PSS/PDDA, PSS/CGG, SC/PDDA, and SC/CGG multilayers as a function of NaCl concentration (C_{NaCl}). For the same layer number, the changes of frequency ($-\Delta f$) and dissipation (ΔD) regarding PSS/PDDA multilayer increase with C_{NaCl}, whereas $-\Delta f$ and ΔD for SC/CGG multilayer increase at C_{NaCl} < 0.1 M and decrease at C_{NaCl} > 0.1 M as C_{NaCl} increases. In the cases of PSS/CGG and SC/PDDA multilayer, for the same layer number, $-\Delta f$ and ΔD increase with C_{NaCl} in the range of C_{NaCl} < 0.5 M, and they decrease with the increasing C_{NaCl} in the case of SC/PDDA multilayer but slightly change for the PSS/CGG multilayer at C_{NaCl} > 0.5 M. QCM-D studies indicate that the growth of multilayers as a function of salt concentration is determined by the delicate balance between the weakening of electrostatic repulsion between identically charged groups and the decrease of electrostatic attraction between neighboring layers. ZPA and AFM measurements demonstrate that the extent of surface charge overcompensation and the surface morphology of the multilayers are controlled by the chain conformation.

INTRODUCTION

Polyelectrolyte multilayer (PEM) has received extensive attention in the past decade due to its promising applications in a wealth of fields such as chemical sensors,[1] optical devices,[2] and biomedical coatings.[3,4] The driving force for the layer-by-layer (LbL) deposition of oppositely charged polyelectrolyte chains is mainly attributed to the electrostatic interactions,[5] though PEM can also be fabricated via the hydrogen bonds[6,7] or covalent chemical bonds.[8,9] It is known that the chain conformation has a significant influence on the multilayer growth because the extent of surface charge overcompensation is governed by the chain conformation on the surface.[10] Generally, the chain conformation of polyelectrolyte is determined not only by the intrinsic properties of chains, e.g., intrinsic chain persistence length,[11] but also by the external conditions including pH,[12] salt concentration,[13,14] as well as salt type.[15,16] Besides, the growth of PEM is also influenced by the chain interpenetration which is related to the chain conformation and the electrostatic interactions.[13,17] For instance, more coiled chain conformation and more strong electrostatic attraction will lead to more strong chain interpenetration.

Our previous studies demonstrated that a higher salt concentration leads to a thicker multilayer in either linear or exponential growth mode when it is fabricated by two flexible polyelectrolytes.[13] It is also reported that the increase of salt concentration is favorable for the multilayer growth regardless of whether it is constructed by flexible or semiflexible

Received: December 30, 2011
Revised: February 14, 2012
Published: February 22, 2012

polyelectrolyte chains.[18−21] Quartz crystal microbalance (QCM) measurements revealed that the thickness of poly(sodium 4-styrenesulfonate) (PSS)/poly(diallyldimethylammonium chloride) (PDDA) multilayer increases with salt concentration.[13,14] The studies on chitosan/heparin multilayer showed that the thickness of the multilayer formed by such two semiflexible polyelectrolytes increases with ionic strength.[20,21] However, recent studies showed that, for the poly(L-lysine)/hyaluronic acid and cationic starch/anionic starch multilayers, the film thickness first increases and then decreases with the increasing salt concentration.[22,23] The mechanism for such an interesting phenomenon is not clear yet. Actually, the nature of the effect of salt concentration on the multilayer growth still remains elusive.

In the growth of a PEM, increasing salt concentration can screen not only the electrostatic attraction between oppositely charged chains from neighboring layers but also the electrostatic repulsion between groups with like charges along the same chain. The former is unfavorable for the multilayer growth due to the decrease of chain interpenetration.[24] In contrast, the latter would give rise to a more coiled conformation of the chains on the surface and thus favor the multilayer growth via increasing the extent of surface charge overcompensation and the chain interpenetration.[17,25,26] Consequently, the effect of salt concentration on the multilayer growth should be determined by the delicate balance between such two opposite factors.

In the present work, by use of a quartz crystal microbalance with dissipation (QCM-D), a zeta potential analyzer (ZPA), and atomic force microscopy (AFM), we have systematically investigated the growth of multilayers which are fabricated by different polyelectrolyte pairs consisting of flexible and semiflexible chains with different intrinsic chain persistence length. We are interested in how the multilayer growth is influenced by the chain conformation, chain interpenetration, and electrostatic interaction at different salt concentrations.

EXPERIMENTAL SECTION

Materials. Poly(sodium 4-styrenesulfonate) (PSS, $M_w \sim 1.0 \times 10^6$ g mol^{-1}), poly(diallyldimethylammonium chloride) (PDDA, $M_w \sim 4.5 \times 10^5$ g mol^{-1}), and poly(ethyleneimine) (PEI, $M_w \sim 2.5 \times 10^4$ g mol^{-1}) were all from Aldrich and were used as received. Cationic guar gum (CGG) was purified to remove insoluble impurities by centrifugation, and then precipitated in ethanol and dried under a vacuum. The M_w of purified CGG determined by laser light scattering is $\sim 1.5 \times 10^6$ g mol^{-1}. Chitosan (deacetylated degree >95%, AR grade, $M_w \sim 3.5 \times 10^5$ g mol^{-1}) from Aladdin was used without further purification. Sulfated chitosan (SC, $M_w \sim 6.2 \times 10^4$ g mol^{-1}) was synthesized from chitosan by a homogeneous sulfation (see the Supporting Information). Sodium chloride (NaCl, AR grade) from Sinopharm was used as received. The water used was purified by filtration through a Millipore Gradient system after distillation, giving a resistivity of 18.2 MΩ cm.

QCM-D Measurements. QCM-D and the AT-cut quartz crystals were from Q-sense AB.[27] The quartz crystal resonator with a fundamental resonant frequency of 5 MHz was mounted in a fluid cell with one side exposed to the solution. The resonator had a mass sensitivity constant (C) of 17.7 ng cm^{-2} Hz^{-1}. The effects of surface roughness were neglected because the resonator surfaces were highly polished with a root-mean-square (RMS) roughness less than 3 nm.[28]

When a quartz crystal is excited to oscillate in the thickness shear mode at its fundamental resonant frequency (f_0) by applying a RF voltage across the electrodes near the resonant frequency, a small layer added to the electrodes induces a decrease in resonant frequency (Δf) which is proportional to the mass change (Δm) of the layer. In vacuum or air, if the added layer is rigid, evenly distributed, and much thinner than the crystal, Δf is related to Δm and the overtone number (n = 1, 3, 5, ...) by the Sauerbrey equation[29]

$$\Delta m = -\frac{\rho_q l_q}{f_0}\frac{\Delta f}{n} = -C\frac{\Delta f}{n} \quad (1)$$

where f_0 is the fundamental frequency and ρ_q and l_q are the specific density and thickness of the quartz crystal, respectively. The dissipation factor is defined by[27]

$$D = \frac{E_d}{2\pi E_s} \quad (2)$$

where E_d is the energy dissipated during one oscillation and E_s is the energy stored in the oscillating system. The measurement of ΔD is based on the fact that the voltage over the crystal decays exponentially as a damped sinusoidal when the driving power of a piezoelectric oscillator is switched off.[27] By switching the driving voltage on and off periodically, we can simultaneously obtain a series of changes of the resonant frequency and the dissipation factor.

The gold-coated resonator was cleaned by using Piranha solution composed of one part H_2O_2 and three parts H_2SO_4 at ~50 °C for ~5 min, rinsed with Milli-Q water, and blown dry with a stream of nitrogen gas. A measurement of LbL deposition was initiated by switching the liquid exposed to the resonator from water to PEI solution with a concentration of 1.0 mg mL^{-1}. PEI is allowed to adsorb onto the resonator surface for ~20 min before rinsing with water to ensure a uniform positively charged coating so that the effects of the substrate on the growth of the multilayer are minimized.[30] After water was replaced with pure NaCl solution, 0.1 mg mL^{-1} polycation and polyanion were alternately introduced into the QCM cell for ~20 min with NaCl solution rinsing in between. Δf and ΔD values from the fundamental overtone were usually noisy because of insufficient energy trapping and thus discarded.[31] Here, all the changes of Δf and ΔD were obtained from the measurements at the third overtone (n = 3) and all the experiments were conducted at 25 ± 0.02 °C. The PEI layer in the pure NaCl solution is set as the zeroth layer. The changes in frequency and dissipation induced by the multilayer growth can be extracted by using each corresponding PEI layer as the reference. From the changes in frequency and dissipation, one can obtain the information about the multilayer thickness, the mass of adsorbed chains, and the conformational change of the polyelectrolyte chains.[32] For example, a larger increase of $-\Delta f$ indicates that more polyelectrolyte chains are adsorbed on the surface to form a thicker multilayer and a larger increase of ΔD implies the formation of a more thick and loose multilayer.[33]

ZPA Measurements. Surface zeta potentials (ζ) of the substrate during LbL deposition were determined using ZPA (Delsa Nano). ζ is obtained according to the Smoluchowski equation[34,35]

$$\zeta = \frac{4\pi\eta U}{\varepsilon} \quad (3)$$

dx.doi.org/10.1021/jp212621h | J. Phys. Chem. B 2012, 116, 3106−3114

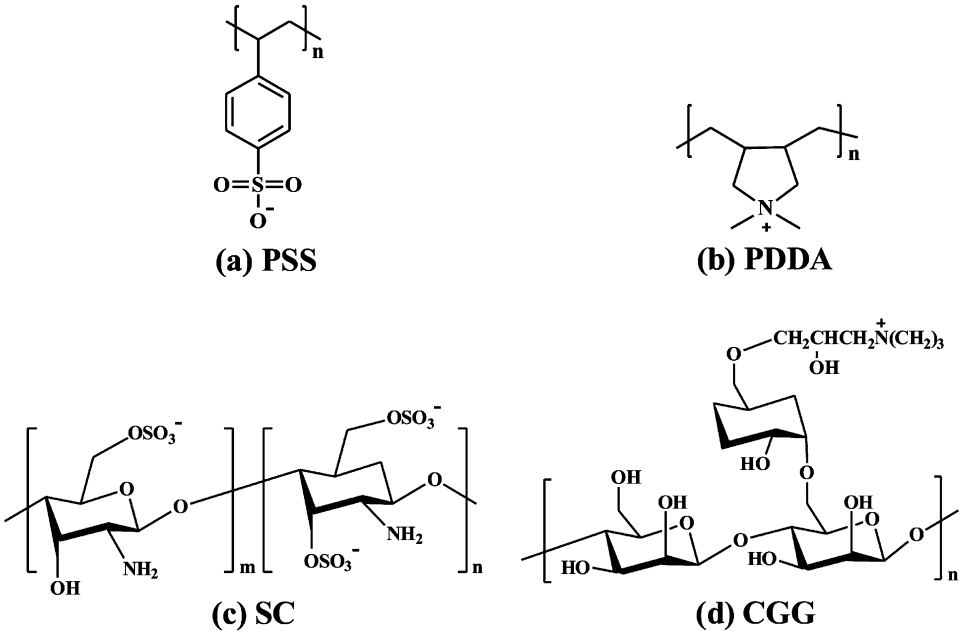

Figure 1. Chemical structures of the four types of polyelectrolytes. (a) Poly(sodium 4-styrenesulfonate) (PSS), (b) Poly(diallyldimethylammonium chloride) (PDDA), (c) Sulfated chitosan (SC), (d) Cationic guar gum (CGG).

where U is the electrophoretic mobility, η is the viscosity of solution, and ε is the dielectric constant of solution.

One can also obtain the surface charge density (σ) from ζ based on the Grahame equation[36]

$$\sigma = \sqrt{8\varepsilon\varepsilon_0 RTc}\,\sinh\left(\frac{zF\zeta}{2RT}\right) \quad (4)$$

where R is the gas constant, T is the temperature, F is the Faraday constant, z is the valence of the counterion, ε_0 is the permittivity of the vacuum, and c is the concentration of the electrolyte solution.

AFM Measurements. Polyelectrolyte multilayer coated surfaces were imaged in air using an AFM (Nanoscope V, Santa Barbara, USA). The root-mean-square (RMS) roughness of the multilayer surface was evaluated from the recorded AFM images. All the AFM measurements were carried out in the tapping mode using standard rectangular silicon cantilevers with a resonance frequency of 150 kHz and a spring constant of 4.5 N m^{-1}. The scanning frequency was 1.0 Hz with a resolution of 512 × 512 pixels.

RESULTS AND DISCUSSION

Generally, the flexible polymers are those for which the contour length is much larger than the persistence length, whereas the semiflexible polymers are those for which the persistence length and the contour length are in the same order of magnitude.[37,38] Figure 1 shows the chemical structures of PSS, PDDA, SC, and CGG. The intrinsic persistence lengths (L_0) of PSS, PDDA, SC, and CGG are ~0.9, ~2.7, ~10.0, and ~10.0 nm, respectively.[39−42] Thus, in the present study, PSS and PDDA are considered as flexible polyelectrolytes,[43,44] whereas SC and CGG are classified as semiflexible polyelectrolytes.[45,46] Since they are all strong polyelectrolytes, the influence of pH fluctuation induced by the addition of salts on the LbL deposition can be neglected.

As we reported before,[13] the increase of salt concentration favors the growth of PSS/PDDA multilayer; namely, both $-\Delta f$ and ΔD increase with NaCl concentration (C_{NaCl}) for the same layer number (Figure 2). Furthermore, the effect of salt

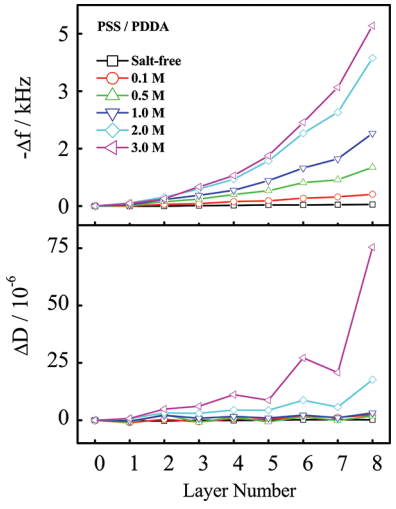

Figure 2. The layer number dependence of shifts in frequency ($-\Delta f$) and dissipation (ΔD) for the PSS/PDDA multilayer as a function of NaCl concentration (C_{NaCl}), where the odd and even layer numbers correspond to the deposition of PSS and PDDA, respectively. This figure is replotted from the Figure 4 in ref 13 with the permission of American Chemical Society.

concentration on the multilayer growth is dominated by chain conformation and chain interpenetration at C_{NaCl} < 1.0 M and $C_{NaCl} \geq$ 1.0 M, respectively.[13] As the salt concentration increases in the range of C_{NaCl} < 1.0 M, the flexible polyelectrolyte chains adopt a more coiled and loopy conformation due to the decrease of electrostatic repulsion between identically charged groups along the same chain. More loops and tails are formed at the polymer/solution interface at a higher salt concentration, leading to a higher extent of surface charge overcompensation during the LbL deposition, which is

dx.doi.org/10.1021/jp212621h | J. Phys. Chem. B 2012, 116, 3106−3114

favorable for the multilayer growth. At C_{NaCl} > 1.0 M, the increase of salt concentration will significantly enhance the extent of chain interpenetration,[13] causing the multilayer to grow exponentially with the layer number based on the "in" and "out" diffusion model.[47] Therefore, as C_{NaCl} increases, $-\Delta f$ and ΔD increase with salt concentration for the same layer number, indicating that the effect of weakening of electrostatic repulsion on the multilayer growth dominates over that of the weakening of electrostatic attraction. In other words, the growth of a multilayer formed by two flexible polyelectrolytes is dominated by the weakening of electrostatic repulsion between the identically charged groups. Note that the polyelectrolyte chain will adopt a quite extended and flat conformation in a salt-free solution due to the strong electrostatic repulsion between identically charged groups along the same chain, which will lead to a low extent of surface charge overcompensation and chain interpenetration, resulting in a thin multilayer film.[13] Therefore, $-\Delta f$ and ΔD slightly increase with layer number in the salt-free solution.

Figure 3 shows the layer number dependence of shifts in frequency $(-\Delta f)$ and dissipation (ΔD) for the SC/CGG multilayer as a function of C_{NaCl}, where the odd and even layer numbers correspond to the deposition of SC and CGG, respectively. In Figure 3a, as C_{NaCl} increases, $-\Delta f$ exhibits two different regimes. For the same layer number, $-\Delta f$ increases with salt concentration in the range of C_{NaCl} < 0.1 M, and then $-\Delta f$ decreases with the increasing salt concentration at C_{NaCl} > 0.1 M. Likewise, ΔD exhibits a similar result. As C_{NaCl} increases, ΔD increases for the same layer number at C_{NaCl} < 0.1 M. When C_{NaCl} is above 0.1 M, ΔD decreases with the increase of salt concentration for the same layer number. Obviously, the salt effect on the growth of SC/CGG multilayer is quite different from that of PSS/PDDA multilayer. Here, the increase of C_{NaCl} favors the growth of SC/CGG multilayer at low salt concentrations, whereas increasing C_{NaCl} is unfavorable for the growth of SC/CGG multilayer at high salt concentrations.

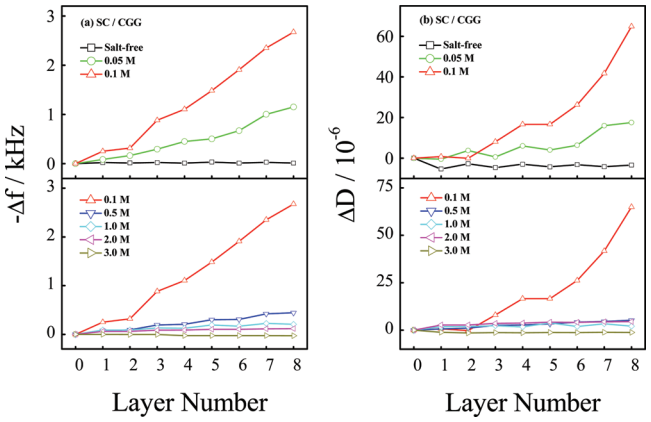

Figure 3. (a) The layer number dependence of shifts in frequency $(-\Delta f)$ for the SC/CGG multilayer as a function of NaCl concentration (C_{NaCl}), (b) The layer number dependence of shifts in dissipation (ΔD) for the SC/CGG multilayer as a function of NaCl concentration (C_{NaCl}). Here, the odd and even layer numbers correspond to the deposition of SC and CGG, respectively.

In general, the conformation of polyelectrolyte is determined by the total chain persistence length (L_p) which represents the effective rigidity of the polyelectrolyte chain.[48] L_p is the sum of L_0 and the electrostatic persistence length (L_e)[49]

$$L_P = L_0 + L_e = L_0 + \frac{l_B \tau^2}{4k^2} \quad (5)$$

where l_B, τ, and k^{-1} are the Bjerrum length, the linear charge density, and the Debye length, respectively. L_0 corresponding to the rigidity of an uncharged chain is independent of the salt concentration.[48] In contrast, L_e arising from the electrostatic repulsion between identically charged groups from the same chain depends on external salt concentration because k^{-1} is inversely proportional to the square root of ionic strength.[50] At low salt concentrations, L_p comes from the contributions of L_0 and L_e. As the salt concentration increases, L_e decreases, leading to a decrease of L_p. Therefore, the polyelectrolyte chains would adopt a more coiled conformation at the polymer/solution interface with salt concentration due to the weakening of electrostatic repulsion between identically charged groups, which favors the multilayer growth by increasing the extent of surface charge overcompensation and chain interpenetration. Meanwhile, the strength of electrostatic attraction between oppositely charged chains from the neighboring layers decreases with the increasing salt concentration, which is unfavorable for the multilayer growth.[24] Clearly, at low salt concentrations, the increase of $-\Delta f$ and ΔD with C_{NaCl} for the same layer number indicates that the growth of SC/CGG multilayer is dominated by the weakening of electrostatic repulsion between identically charged groups.

When C_{NaCl} is above 0.1 M, the L_e values of SC and CGG are, respectively, less than 0.26 and 0.05 nm calculated from eq 5; that is, L_e is much smaller than L_0 for such two semiflexible polyelectrolytes. Thus, as C_{NaCl} increases, the contribution of L_e to L_p can be neglected and L_p would keep almost constant with C_{NaCl}. Consequently, the chain conformation and the extent of surface charge overcompensation slightly change with C_{NaCl} even though the electrostatic repulsion is gradually screened by the added salts. On the other hand, the electrostatic attraction between the neighboring layers is also screened with the increase of C_{NaCl}, which is unfavorable for the multilayer growth due to the decrease of chain interpenetration. Clearly, the fact that $-\Delta f$ and ΔD decrease with salt concentration for the same layer number indicates that the effect of weakening of electrostatic attraction on the multilayer growth dominates over that of the weakening of electrostatic repulsion. In other words, the growth of SC/CGG multilayer is dominated by the weakening of electrostatic attraction between the neighboring layers at the high salt concentrations.

The linear growth of SC/CGG multilayer with weak chain interpenetration may form a stratified film-like structure,[5] whereas the exponential growth of PSS/PDDA multilayer with a high extent of chain interpenetration at the high salt concentrations may form meshed film-like structure.[23] Nevertheless, the precise characterization of multilayer microstructure needs more detailed investigations with other techniques, e.g., X-ray reflectivity.[5] It is also worth noting that the hydrogen bonding between $-NH_2$ and $-OH$ groups may contribute to the growth of SC/CGG multilayer. However, the strength of hydrogen bonding is independent of the salt concentration;[51] that is, the effect of hydrogen bonding on the multilayer growth at different salt concentrations can be neglected.

What will happen if the multilayer is constructed by a flexible/semiflexible polyelectrolyte pair? Figure 4 shows the

dx.doi.org/10.1021/jp212621h | J. Phys. Chem. B 2012, 116, 3106–3114

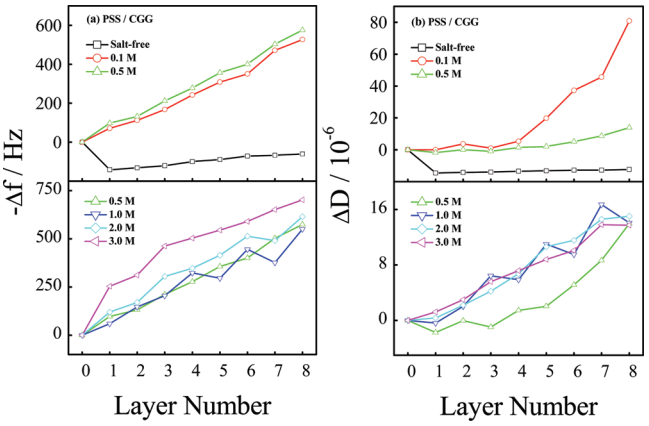

Figure 4. (a) The layer number dependence of shifts in frequency ($-\Delta f$) for the PSS/CGG multilayer as a function of NaCl concentration (C_{NaCl}), (b) The layer number dependence of shifts in dissipation (ΔD) for the PSS/CGG multilayer as a function of NaCl concentration (C_{NaCl}). Here, the odd and even layer numbers correspond to the deposition of PSS and CGG, respectively.

layer number dependence of shifts in frequency ($-\Delta f$) and dissipation (ΔD) for PSS/CGG multilayer as a function of C_{NaCl}, where the odd and even layer numbers correspond to the deposition of PSS and CGG, respectively. For the same layer number, $-\Delta f$ increases with the salt concentration in the range of C_{NaCl} < 0.5 M and keeps almost constant with the salt concentration at C_{NaCl} > 0.5 M. On the other hand, for the same layer number, ΔD increases with the salt concentration when C_{NaCl} is below 0.5 M except that in the case of 0.1 M, but ΔD keeps almost constant with the salt concentration when C_{NaCl} is above 0.5 M. The rapid increase of ΔD with the layer number at C_{NaCl} of 0.1 M might be attributed to the formation of a loose multilayer which strongly damps the shear wave.[33] The PSS chains would be more collapsed and less hydrated at C_{NaCl} of 0.5 M than that at C_{NaCl} of 0.1 M, so that PSS and CGG chains may form a looser multilayer at C_{NaCl} of 0.1 M with more water molecules trapped per unit thickness. This proposition can be further indicated by the fact that the ΔD vs $-\Delta f$ plot at C_{NaCl} of 0.1 M has a larger slope than that at C_{NaCl} of 0.5 M (see Figure S3 in the Supporting Information). Therefore, ΔD exhibits a more rapid increase with the layer number at C_{NaCl} of 0.1 M than that at C_{NaCl} of 0.5 M, though $-\Delta f$ exhibits an opposite phenomenon.

$-\Delta f$ and ΔD increase with C_{NaCl} for the same layer number at C_{NaCl} < 0.5 M, indicating that the growth of PSS/CGG multilayer is dominated by the decrease of electrostatic repulsion between identically charged groups. This result is similar to that of the PSS/PDDA and SC/CGG multilayers at low salt concentrations. When C_{NaCl} is above 0.5 M, the L_e values of PSS and CGG are less than 0.39 and 0.01 nm, respectively. Thus, at C_{NaCl} > 0.5 M, L_p of CGG slightly changes with C_{NaCl} because L_e is much smaller than L_0 (~10 nm). That is, the extent of surface charge overcompensation induced by the adsorption of CGG chains slightly changes with salt concentration. However, the decrease of L_e of PSS chains with the increasing C_{NaCl} in the range of C_{NaCl} > 0.5 M would lead to a decrease of L_p, since the L_e is comparable to the L_0 (~0.9 nm), so that PSS chains adopt a more coiled conformation and stronger surface charge overcompensation results at a higher salt concentration. Note that the electrostatic attraction between the neighboring layers always decreases with the increasing salt concentration. Consequently, as C_{NaCl} increases, the growth of PSS/CGG multilayer at C_{NaCl} > 0.5 M is determined by the delicate balance between the decrease of electrostatic repulsion between the identically charged groups on the PSS chains and the weakening of electrostatic attraction between the neighboring layers. The fact that $-\Delta f$ and ΔD slightly vary with C_{NaCl} for the same layer number indicates that such two opposite effects offset each other at the high salt concentrations. From the viewpoint of chain interpenetration, the increase of salt concentration at C_{NaCl} < 0.5 M leads to a more coiled conformation and more strong chain interpenetration, favoring the PSS/CGG multilayer growth. When C_{NaCl} is above 0.5 M, the decrease of electrostatic repulsion between the identically charged groups on the PSS chains and the weakening of electrostatic attraction between the neighboring layers may make the chain interpenetration slightly change, so that $-\Delta f$ and ΔD slightly change with C_{NaCl} for the same layer number.

For the same layer number in the growth of SC/PDDA multilayer, $-\Delta f$ and ΔD increase with the salt concentration in the range of C_{NaCl} < 0.5 M and decrease with the increasing salt concentration at C_{NaCl} > 0.5 M (Figure 5). This observation is

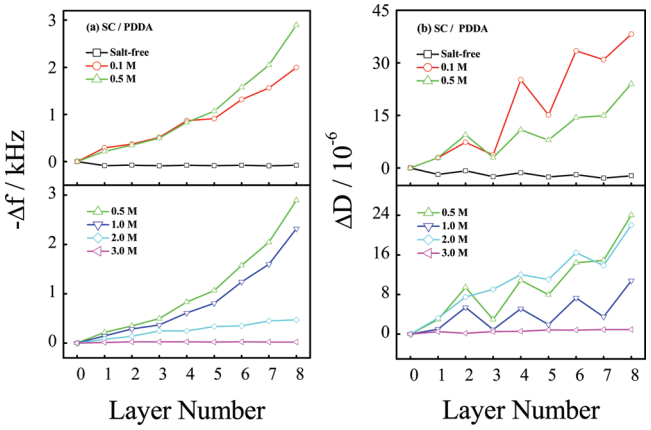

Figure 5. (a) The layer number dependence of shifts in frequency ($-\Delta f$) for the SC/PDDA multilayer as a function of NaCl concentration (C_{NaCl}); (b) the layer number dependence of shifts in dissipation (ΔD) for the SC/PDDA multilayer as a function of NaCl concentration (C_{NaCl}). Here, the odd and even layer numbers correspond to the deposition of SC and PDDA, respectively.

similar to that of the SC/CGG multilayer. At the low salt concentrations, the increase of C_{NaCl} causes stronger surface charge overcompensation and chain interpenetration due to the decrease of L_e of SC and PDDA chains, thereby favoring the multilayer growth. In addition, the large increase of ΔD with the layer number in the case of 0.1 M might also relate to the formation of a loose multilayer. When C_{NaCl} is above 0.5 M, L_e of SC and PDDA are less than 0.05 and 0.03 nm, respectively. As C_{NaCl} increases, L_p for both SC and PDDA chains slightly changes because L_e is much smaller than the corresponding L_0. As a result, the chain conformation and the extent of surface charge overcompensation slightly change with C_{NaCl}. Meanwhile, the weakening of electrostatic attraction between the neighboring layers will result in a decrease of chain interpenetration with salt concentration. $-\Delta f$ and ΔD decrease with increasing salt concentration at C_{NaCl} > 0.5 M for the same layer number, indicating that the growth of SC/PDDA multilayer is

dx.doi.org/10.1021/jp212621h | J. Phys. Chem. B 2012, 116, 3106–3114

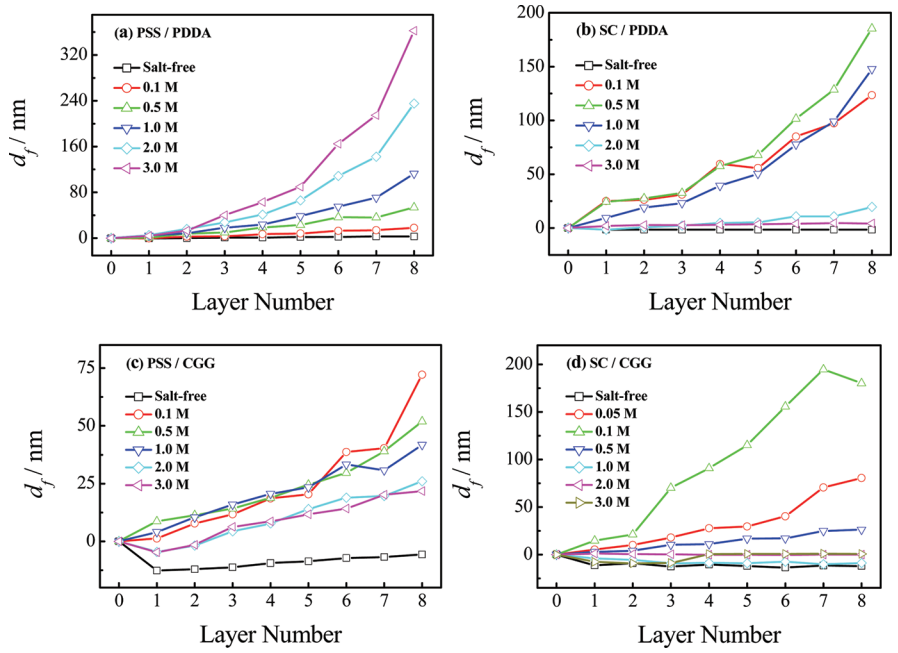

Figure 6. The layer number dependence of hydrodynamic thickness (d_f) as a function of NaCl concentration (C_{NaCl}) fit by the Voigt model based on the changes of Δf and ΔD at n = 3, 5, and 7. Here, the odd and even layer numbers correspond to the deposition of polyanion and polycation, respectively. (a) PSS/PDDA, (b) SC/PDDA, (c) PSS/CGG, and (d) SC/CGG. Part a is replotted from the Figure 6 in ref 13 with the permission of American Chemical Society.

Scheme 1. Schematic Illustration for the Changes of Hydrodynamic Thickness (d_f) of the Four Types of Polyelectrolyte Multilayers with the Increasing NaCl Concentration (C_{NaCl})

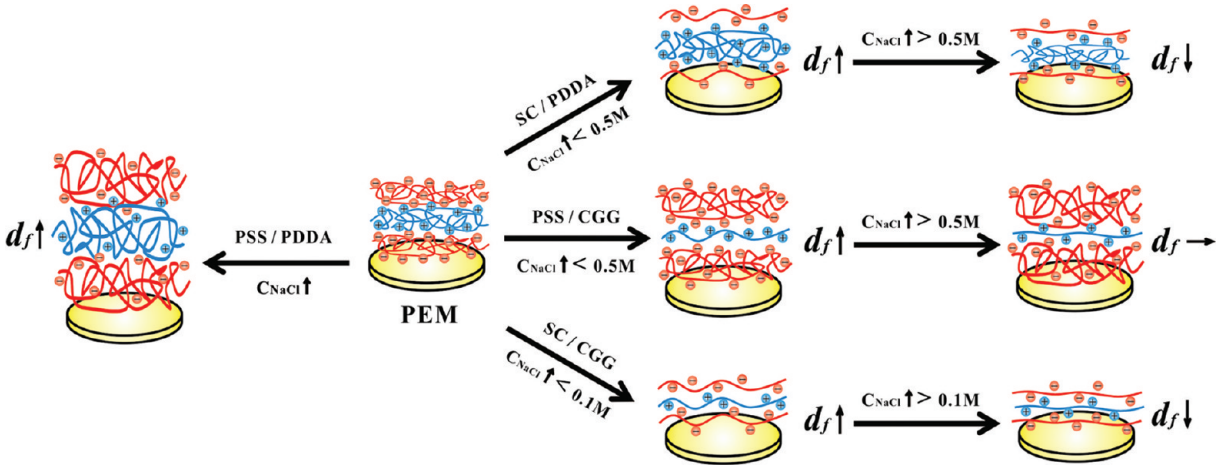

dominated by the weakening of electrostatic attraction between the neighboring layers at the high salt concentrations.

The layer number dependence of hydrodynamic thickness (d_f) of the four types of multilayers at different C_{NaCl} was fit using the Voigt model (Figure 6). For the same layer number, d_f increases with C_{NaCl} in the growth of PSS/PDDA multilayer, but d_f of SC/PDDA multilayer increases with the salt concentration in the range of C_{NaCl} < 0.5 M and decreases with the increasing salt concentration in the range of C_{NaCl} > 0.5 M. In the case of PSS/CGG multilayer, for the same layer number, d_f increases with the salt concentration in the range of C_{NaCl} < 0.5 M. In the range of C_{NaCl} > 0.5 M, for the same layer number, d_f of PSS/CGG multilayer at C_{NaCl} of 2.0 M is similar to that at 3.0 M, and is a little smaller than that at 1.0 M. In the case of SC/CGG multilayer, d_f for the same layer number increases with the salt concentration in the range of C_{NaCl} < 0.1 M and decreases with the increasing salt concentration in the range of C_{NaCl} > 0.1 M. Due to the participation of flexible chains in the formation of PEM, C_{NaCl} at the transition point of d_f changes from 0.1 M for the SC/CGG multilayer to 0.5 M for the PSS/CGG or SC/PDDA multilayer. Obviously, the changes of d_f agree with the observations in Figures 2, 3, 4, and 5.

Scheme 1 illustrates the changes of d_f for the four types of multilayers with the increasing C_{NaCl}. Clearly, the flexible/semiflexible and semiflexible/semiflexible multilayers have a threshold concentration above which d_f decreases or slightly changes with salt concentration. Below the threshold concentration, d_f increases with salt concentration, similar to the case of the flexible/flexible multilayer. Our previous study demonstrated that d_f of the flexible/flexible multilayer increases monotonously with salt concentration until the salt concentration reaches a critical value.[17] Above the critical salt

dx.doi.org/10.1021/jp212621h | J. Phys. Chem. B 2012, 116, 3106–3114

concentration, the polyelectrolyte chains cannot form a multilayer on a solid surface because the formation of a multilayer will lead to a substantial loss of chain conformational entropy.[17] Thus, there is no threshold concentration for the flexible/flexible multilayer.

It is known that the conformation of polyelectrolyte chains on a surface significantly influences the extent of surface charge overcompensation, thereby determining the magnitude of ζ and σ.[52−54] Figure 7 shows the changes in ζ and σ as a function of

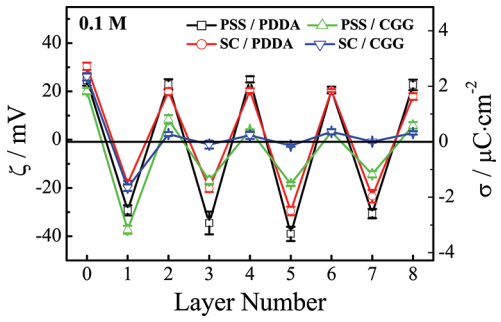

Figure 7. The layer number dependence of changes in surface zeta potential (ζ) and surface charge density (σ) for the four types of multilayers at a NaCl concentration (C_{NaCl}) of 0.1 M. Here, the odd and even layer numbers correspond to the deposition of polyanion and polycation, respectively.

layer number for the four types of multilayers at C_{NaCl} of 0.1 M, where the odd and even layer numbers correspond to the deposition of polyanion and polycation, respectively. It is evident that ζ and σ exhibit periodic changes along with the layer number. The initially positive ζ (~25 mV) is attributed to the presence of the PEI layer on the surface. The adsorption of PSS on the PEI surface causes ζ to decrease to ~ −30 mV for the PSS/PDDA and PSS/CGG multilayers, and the adsorption of SC on PEI surface causes ζ to decrease to ~ −20 mV for the SC/PDDA and SC/CGG multilayers. Meanwhile, σ changes from ~2.2 μC·cm^{-2} to ~ −2.6 μC·cm^{-2} for the PSS/PDDA and PSS/CGG multilayers and changes from ~2.2 μC·cm^{-2} to ~ −1.6 μC·cm^{-2} for the SC/PDDA and SC/CGG multilayers. The magnitude of ζ or σ reflects the extent of surface charge overcompensation. Specifically, a more negative value of ζ or σ after adsorbing negatively charged chains on the PEI surface indicates more strong surface charge overcompensation. Thus, the adsorbed PSS chains can form a more coiled conformation than the SC chains on the surface, resulting in a higher extent of surface charge overcompensation. The following adsorption of positively charged chains makes the surface charge reverse again. For example, ζ after the adsorption of PDDA and CGG are ~20 and 4 mV, respectively, and σ for the PDDA and CGG surfaces are ~1.8 and ~0.4 μC·cm^{-2}, respectively. This fact indicates that the adsorption of PDDA chains leads to stronger surface charge overcompensation than the CGG chains because the former can form a more coiled and loopy conformation than the latter on the surface.

For all the even layer numbers, the adsorption of PDDA gives rise to relatively large values of ζ and σ than that of the CGG chains, indicating that the PDDA chains form a more coiled conformation with a higher extent of surface charge overcompensation than that of the CGG chains. On the other hand, for the odd layer numbers with the exception of the first layer, the adsorption of PSS in the growth of PSS/PDDA multilayer results in the largest absolute values of ζ and σ and the adsorption of SC in the growth of SC/CGG multilayer leads to the smallest absolute values of ζ and σ, indicating that the PSS chains form more coiled conformation with stronger surface charge overcompensation than that of the SC chains. Interestingly, the adsorption of PSS chains in the growth of PSS/CGG multilayer and the adsorption of SC chains in the growth of SC/PDDA multilayer exhibit similar values of ζ and σ. This is probably because the relatively low values of ζ and σ for the CGG surface reduce the extent of surface charge overcompensation of the following deposition layer (i.e., PSS) and the relatively large values of ζ and σ for the PDDA surface enhance the extent of surface charge overcompensation of the following deposition layer (i.e., SC). Eventually, the PSS surface in PSS/CGG multilayer and the SC surface in SC/PDDA multilayer have similar extents of surface charge overcompensation and similar values of ζ and σ.

Figure 8 shows the surface morphologies and RMS roughness of the four types of multilayers observed by AFM. The surface morphology of the multilayer can provide some useful information on the conformation of polyelectrolyte chains on the surface.[55,56] As shown in Figure 8a, the PSS/PDDA multilayer exhibits a quite rough surface (RMS roughness ~5.1 nm) with some granular structures. When C_{NaCl} is 0.1 M, k^{-1} is ~1 nm based on the equation $k^{-1} = 0.3$ nm/$\sqrt{I}$ for the monovalent ions.[55] Thus, the flexible PSS and PDDA chains would adopt random coil configurations on the surface, and the complexation of PSS and PDDA chains would form a rough surface during the multilayer growth. However, the multilayers formed by other polycation−polyainon pairs exhibit quite flat surfaces, as reflected by the fact that the RMS roughness for SC/PDDA, PSS/CGG, and SC/CGG multilayers are ~1.6, ~1.5, and ~1.4 nm, respectively. This is because at least one semiflexible polyelectrolyte participates in the formation of these multilayers. The semiflexible polyelectrolyte with a large L_0 would form a flat conformation on the surface, thereby giving rise to a smooth multilayer surface regardless of the rigidity of the oppositely charged counterpart. The AFM results are consistent with those from QCM-D and ZPA measurements.

CONCLUSION

By use of QCM-D, ZPA, and AFM, we have investigated the growth of multilayers formed by flexible and semiflexible polyelectrolytes. Our study demonstrates that the growth of polyelectrolyte multilayers with salt concentration is determined by the delicate balance between the weakening of electrostatic repulsion between the identically charged groups and the decrease of electrostatic attraction between the neighboring layers. For the flexible/flexible polyelectrolyte pair, the multilayer growth is dominated by the weakening of electrostatic repulsion between the identically charged groups with the increasing salt concentration. For other polyelectrolyte pairs, the multilayer growth exhibits two different regimes. For example, in the cases of semiflexible/flexible and semiflexible/semiflexible polyelectrolyte pairs, as the salt concentration increases, the multilayer growth is dominated by the weakening of electrostatic repulsion between the identically charged groups and by the decrease of electrostatic attraction between the neighboring layers at the low and high salt concentrations, respectively. Our results also indicate that the extent of surface charge overcompensation, the chain interpenetration, and the surface roughness of the multilayers are significantly influenced by the chain conformation on the surface.

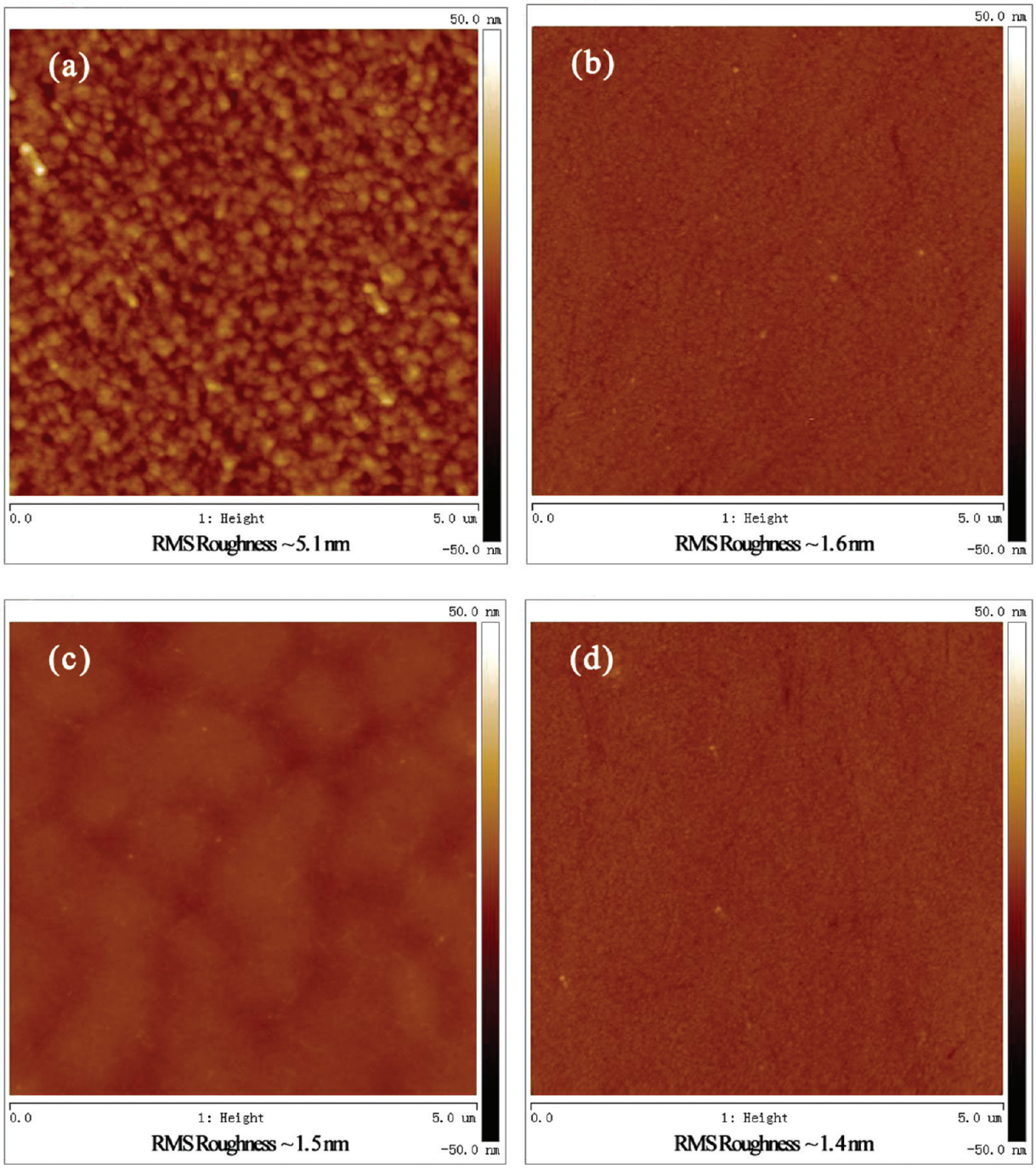

Figure 8. The surface morphologies and RMS roughness of the four types of multilayers (4-bilayers) obtained by AFM in air after drying from 0.1 M NaCl solution: (a) PSS/PDDA, (b) SC/PDDA, (c) PSS/CGG, and (d) SC/CGG.

■ ASSOCIATED CONTENT

Ⓢ Supporting Information

The synthesis of sulfated chitosan, the corresponding characterization of sulfated chitosan by FTIR and ^{13}C NMR, and the ΔD vs $-\Delta f$ plot for PSS/CGG multilayer. This material is available free of charge via the Internet at http://pubs.acs.org.

■ AUTHOR INFORMATION

Corresponding Author

*E-mail: gml@ustc.edu.cn.

Notes

The authors declare no competing financial interest.

■ ACKNOWLEDGMENTS

The financial support of National Program on Key Basic Research Project (2012CB933802), the National Natural Science Foundation of China (21004058, 91127042), the National Distinguished Young Investigator Fund (20725414), Scientific Research Startup Foundation of the Chinese Academy of Sciences, and the Fundamental Research Funds for the Central Universities is acknowledged.

■ REFERENCES

(1) Hoshi, T; Saiki, H; Kuwazawa, S; Tsuchiya, C; Chen, Q; Anzai, J. *Anal. Chem.* **2001**, *73*, 5310−5315.

(2) Nolte, A. J.; Rubner, M. F.; Cohen, R. E. *Langmuir* **2004**, *20*, 3304−3310.
(3) Boulmedais, F.; Frisch, B.; Etienne, O.; Lavalle, P.; Picart, C.; Ogier, J.; Voegel, J. -C.; Schaaf, P.; Egles, C. *Biomaterials* **2004**, *25*, 2003−2011.
(4) Boudou, T.; Crouzier, T.; Ren, K. F.; Blin, G.; Picart, C. *Adv. Mater.* **2010**, *22*, 441−467.
(5) Decher, G. *Science* **1997**, *277*, 1232−1237.
(6) Wang, L. Y.; Wang, Z. Q.; Zhang, X.; Shen, J. C.; Chi, L. F.; Fuchs, H. *Macromol. Rapid Commun.* **1997**, *18*, 509−514.
(7) Sukhishvili, S. A.; Granick, S. *Macromolecules* **2002**, *35*, 301−310.
(8) Such, G. K.; Quinn, J. F.; Quinn, A.; Tjipto, E.; Caruso, F. *J. Am. Chem. Soc.* **2006**, *128*, 9318−9319.
(9) Tang, Y. C.; Liu, G. M.; Yu, C. Q.; Wei, X. L.; Zhang, G. Z. *Langmuir* **2008**, *24*, 8929−8933.
(10) Schoeler, B.; Kumaraswamy, G.; Caruso, F. *Macromolecules* **2002**, *35*, 889−897.
(11) Dobrynin, A. V.; Rubinstein, M. *Prog. Polym. Sci.* **2005**, *30*, 1049−1118.
(12) Sukhorukov, G. B.; Antipov, A. A.; Voigt, A; Donath, E; Möhwald, H. *Macromol. Rapid Commun.* **2001**, *22*, 44−46.
(13) Liu, G. M.; Zou, S. R.; Fu, L.; Zhang, G. Z. *J. Phys. Chem. B* **2008**, *112*, 4167−4171.
(14) Guzmán, E.; Ritacco, H.; Rubio, J. E. F.; Rubio, R. G.; Ortega, F. *Soft Matter* **2009**, *5*, 2130−2142.
(15) Wong, J. E.; Zastrow, H.; Jaeger, W.; von Klitzing, R. *Langmuir* **2009**, *25*, 14061−14070.
(16) Liu, G. M.; Hou, Y.; Xiao, X; Zhang, G. Z. *J. Phys. Chem. B* **2010**, *114*, 9987−9993.
(17) Liu, G. M.; Zhao, J. P.; Sun, Q. Y.; Zhang, G. Z. *J. Phys. Chem. B* **2008**, *112*, 3333−3338.
(18) Dubas, S. T.; Schlenoff, J. B. *Macromolecules* **1999**, *32*, 8153−8160.
(19) Lösche, M.; Schmitt, J.; Decher, G.; Bouwman, W. G.; Kjaer, K. *Macromolecules* **1998**, *31*, 8893−8906.
(20) Boddohi, S.; Killingsworth, C. E.; Kipper, M. J. *Biomacromolecules* **2008**, *9*, 2021−2028.
(21) Lundin, M.; Solaqa, F.; Thormann, E.; Macakova, L.; Blomberg, E. *Langmuir* **2011**, *27*, 7537−7548.
(22) Johansson, E.; Lundström, L.; Norgren, M.; Wågberg, L. *Biomacromolecules* **2009**, *10*, 1768−1776.
(23) Mjahed, H.; Cado, G.; Boulmedais, F.; Senger, B.; Schaaf, P.; Ball, V.; Voegel, J. C. *J. Mater. Chem.* **2011**, *21*, 8416−8421.
(24) Von Klitzing, R.; Wong, J. E.; Jaeger, W.; Steitz, R. *Curr. Opin. Colloid Interface Sci.* **2004**, *9*, 158−162.
(25) Schlenoff, J.; Ly, H.; Li, M. *J. Am. Chem. Soc.* **1998**, *120*, 7626−7634.
(26) Schlenoff, J. B.; Dubas, S. T. *Macromolecules* **2001**, *34*, 592−598.
(27) Rodahl, M.; Höök, F.; Krozer, A.; Kasemo, B.; Breszinsky, P. *Rev. Sci. Instrum.* **1995**, *66*, 3924−3930.
(28) Martin, S. J.; Frye, G. C.; Ricco, A. J.; Senturia, S. D. *Anal. Chem.* **1993**, *65*, 2910−2922.
(29) Sauerbrey, G. *Z. Phys.* **1959**, *155*, 206−222.
(30) Poptoshev, E.; Schoeler, B.; Caruso, F. *Langmuir* **2004**, *20*, 829−834.
(31) Bottom, V. E. *Introduction to Quartz Crystal Unit Design*; Van Nostrand Reinhold Co.: New York, 1982.
(32) Zhang, G. Z.; Wu, C. *Macromol. Rapid Commun.* **2009**, *30*, 328−335.
(33) Voinova, M. V.; Rodahl, M.; Jonson, M.; Kasemo, B. *Phys. Scr.* **1999**, *59*, 391−396.
(34) Henry, D. C. *Proc. R. Soc. London* **1931**, *133*, 106.
(35) Hozumi, A.; Sugimura, H.; Yokogawa, Y.; Kameyama, T.; Takai, O. *Colloids Surf., A* **2001**, *182*, 257−261.
(36) Calero, C.; Faraudo, J.; Bastos-González. *J. Am. Chem. Soc.* **2011**, *133*, 15025−15035.
(37) HA, B. -Y.; Thirumalai, D. *Macromolecules* **1995**, *28*, 577−581.
(38) Netz, R. R.; Andelman, D. *Phys. Rep.* **2003**, *380*, 1−95.
(39) Brûlet, A.; Boué, F.; Cotton, J. P. *J. Phys. II* **1996**, *6*, 885−891.
(40) Mattison, K. W.; Dubin, P. L.; Brittain, I. J. *J. Phys. Chem. B* **1998**, *102*, 3830−3836.
(41) Rinaudo, M. *Macromol. Biosci.* **2006**, *6*, 590−610.
(42) Morris, G. A.; Patel, T. R.; Picout, D. R.; Ross-Murphy, S. B.; Ortega, A.; de la Torre, J. G.; Harding, S. E. *Carbohydr. Polym.* **2008**, *72*, 356−360.
(43) Schiessel, H. *Macromolecules* **1999**, *32*, 5673−5680.
(44) Alatorre-Meda, M.; Taboada, P.; Krajewska, B.; Willemeit, M.; Deml, A.; Klosel, R.; Rodriguez, J. R. *J. Phys. Chem. B* **2010**, *114*, 9356−9366.
(45) Weinhold, M. X.; Thoming, J. *Carbohydr. Polym.* **2011**, *84*, 1237−1243.
(46) Patel, T. R.; Picout, D. R.; Ross-Murphy, S. B.; Harding, S. E. *Biomacromolecules* **2001**, *2*, 1301−1309.
(47) Lavalle, P.; Picart, C.; Mutterer, J.; Gergely, C.; Reiss, H.; Voegel, J. C.; Senger, B.; Schaaf, P. *J. Phys. Chem. B* **2004**, *108*, 635−648.
(48) Schönhoff, M. *J. Phys.: Condens. Matter* **2003**, *15*, R1781−R1808.
(49) Dobrynin, A. V. *Macromolecules* **2005**, *38*, 9304−9314.
(50) Solomon, T. *J. Chem. Educ.* **2001**, *78*, 1691−1692.
(51) Scholtz, J. M.; Qian, H.; Robbins, V. H.; Baldwin, R. L. *Biochemistry* **1993**, *32*, 9668−9676.
(52) Dahlgren, M. A. G. *Langmuir* **1994**, *10*, 1580−1583.
(53) Voigt, U.; Jaeger, W.; Findenegg, G. H.; Klitzing, R. V. *J. Phys. Chem. B* **2003**, *107*, 5273−5280.
(54) Nishida, I.; Okaue, Y.; Yokoyama, T. *Langmuir* **2010**, *26*, 11663−11669.
(55) McAloney, R. A.; Sinyor, M.; Dudnik, V.; Goh, M. C. *Langmuir* **2001**, *17*, 6655−6663.
(56) McAloney, R. A.; Dudnik, V.; Goh, M. C. *Langmuir* **2003**, *19*, 3947−3952.